HHS Public Access

Author manuscript

Science. Author manuscript; available in PMC 2015 December 16.

Published in final edited form as:

Science. 2015 August 21; 349(6250): 882–885. doi:10.1126/science.aab1478.

Structures of the RNA polymerase-σ^{54} reveal new and conserved regulatory strategies

Yun Yang[1,4,+], **Vidya C. Darbari**[1,2,+], **Nan Zhang**[3], **Duo Lu**[1,5], **Robert Glyde**[1,2], **Yiping Wang**[4], **Jared Winkelman**[6], **Richard L. Gourse**[6], **Katsuhiko S. Murakami**[7], **Martin Buck**[3], and **Xiaodong Zhang**[1,2,*]

[1]Centre for Structural Biology, Imperial College London, South Kensington, SW7 2AZ, UK

[2]Department of Medicine, Imperial College London, South Kensington, SW7 2AZ, UK

[3]Department of Life Sciences, Imperial College London, South Kensington, SW7 2AZ, UK

[4]State Key Laboratory of Protein and Plant Gene Research, College of Life Sciences, Peking University, China

[6]Department of Bacteriology, University of Wisconsin-Madison, Madison, WI53706, USA

[7]Department of Biochemistry and Molecular Biology, Center for RNA Molecular Biology, Pennsylvania State University, University Park, PA 16802, USA

Abstract

Transcription by RNA polymerase in bacteria requires specific promoter recognition by σ factors. The major variant σ factor (σ^{54}) initially forms a transcriptionally silent complex requiring specialised ATP-dependent activators for initiation. Our crystal structure of the 450 kDa RNAP-σ^{54} holoenzyme at 3.8 Å reveals molecular details of σ^{54} and its interactions with RNAP. The structure explains how σ^{54} targets different regions in RNAP to exert its inhibitory function. Although σ^{54} and the major σ factor, σ^{70}, have similar functional domains and contact similar regions of RNAP, unanticipated differences are observed in their domain arrangement and interactions with RNAP, explaining their distinct properties. Furthermore, we observe evolutionarily conserved regulatory hotspots in RNAPs that can be targeted by a diverse range of mechanisms to fine tune transcription.

Gene transcription is a tightly regulated event. A range of factors are required to maintain RNAP in a signal responsive, but inhibited state and to target it to specific genes (1). Bacterial sigma (σ) factors, eukaryotic TFIIB and other general transcription factors, are the primary promoter recruitment factors. The major variant σ^{54} (also called σ^{N}) is utilised in

*Correspondence should be addressed to: Xiaodong.zhang@imperial.ac.uk, +44 (0)207 5943151.

[5]current address: State Key Laboratory of Bioactive Substance and Function of Natural Medicine, Institute of Material Medicine, Chinese Academy of Medical Sciences & Peking Union Medical College, China

[+]These authors contributed equally to this work

Supplementary Materials

Materials and Methods

Figs. S1 to S5

Tables S1

References (31-43)

transcribing genes for numerous stress responses (2). Unlike the major σ^{70} class, which recognises the -35 and -10 promoter DNA elements, the σ^{54} class directs RNAP to promoter sites through the -24 and -12 DNA elements and forms a stable closed promoter complex that is unable to spontaneously melt DNA and initiate transcripts (3). Instead, the initiation process requires ATP-dependent activator proteins bound to upstream enhancer sites to actively remodel the RNAP-σ^{54}-DNA complex (4).

σ^{54} contains four structural domains connected by long coils and loops that span a large area of the RNAP core enzyme, which consists of two α, β, β' and ω subunits (5, 6) (Fig. 1A-C, Fig. S1A-B, Table S1). σ^{54} Region I (RI, residues 1-56) forms a hook comprised of two α-helices. Region II (RII, residues 57-120) also contains two α-helices (residues 57-85) in addition to loops that are buried inside the RNAP (Fig. 1A, 1C). The RNAP core-binding domain (CBD) of σ^{54} extends as a structural fold to residue 250 and consists of two α-helical subdomains. Following on from the CBD, the backbone extends back to connect to a loop region, before an extra long α-helix (residues 315-353, hereafter called ELH, spanning 50 Å) followed by the HTH domain (residues 365 – 385), involved in interaction with the -12 promoter elements (3). The domain containing the RpoN box (RpoN domain), responsible for recognizing the -24 promoter elements, consists of a three-helical bundle (residues 415 – 477) (Fig. 1A) (3). The σ^{54} polypeptide chain snakes back and forth through its loop regions embedded in the RNAP. We carried out crosslinking experiments between σ^{54} and RNAP in solution using a *p*-benzoyl-L-phenylalanine-incorporated RNAP library. The amino acids that are crosslinked to σ^{54} agree well with the RNAP-σ^{54} crystal structure (Fig. 1D yellow, Fig. S1C).

We crystallized RNAP-σ^{54} in complex with a 28 bp DNA containing the -24 and -12 promoter elements. The crystals diffracted to 8 Å resolution, with the electron density for DNA being unambiguous (Fig. 1E), and the molecular envelope for the holoenzyme clear. We thus constructed a structural model of RNAP-σ^{54}-DNA (Fig. 1E, Fig. S1D).

All σ factors contain a major RNAP core-binding domain (CBD) and a major DNA binding domain, recognising either the -35 or -24 elements. The CBD of σ^{54} (Fig. 1A) binds towards the upstream face of the RNAP (Fig. 1C, based on promoter DNA binding orientation) making extensive interactions with many functional modules within the RNAP including the β-flap (residues 835-937), the C-terminus of the β subunit (residues 1267 – 1320), the β' zipper/Zn-binding domain (residues 35-100), the β' dock domain (residues 370-420) as well as the α subunit carboxyl terminal domain (α-CTD) (Fig. 2A). Using FeBABE cleavage assays, residue 198 of σ^{54} (within the CBD) can indeed be mapped to a region within the β-flap (7).

The RpoN domain of σ^{54} is the most conserved domain among σ^{54} from different organisms (Fig. S2). This domain extends from the main body of RNAP and does not contact other parts of σ^{54} nor core enzyme (Fig. 1A, 1C). Instead, it interacts with an adjacent RNAP molecule in the crystal, suggesting that its location is flexible in solution. In the RNAP-σ^{54}-DNA complex model, the RpoN domain is indeed moved relative to the RNAP-σ^{54} structure (Fig. S1D). Unlike the flexible RpoN domain, the RIII-HTH domain of σ^{54}, which binds to the -12 promoter region, stably associates with the RNAP core through RI-RIII (Fig. 1E,

Fig. S1D) (8-10). Our data thus suggest that -12 binding is a major functional determinant for σ^{54} holoenzyme promoter recognition as well as stable closed complex formation.

The σ^{54} RI plays an inhibitory role and contains contact sites for its cognate activator proteins (11, 12). RI interacts with RIII, forming a structural module that lies along the cleft between β and β' (Fig. 1C and Fig. 2B), where template strand DNA enters the active site cleft (13). Our structure clearly suggests that the entry of promoter DNA into RNAP is blocked by RI and RIII of σ^{54}. Fitting of the RNAP-σ^{54} crystal structure into the cryo-EM map of activator bound RNAP-σ^{54} holoenzyme (14) positions the RI helices inside the connecting density leading to the activator protein, indicating that RI in the RNAP-σ^{54} structure is presented favourably to contact the activator (Fig. S3A).

RII penetrates deeply into the DNA binding channel (Fig. 1, Fig. 2C-D). RII can be divided into three sub-regions based on their locations in the holoenzyme. RII.1 (residues 57-85) occupies the downstream DNA-binding cleft of RNAP, just above the bridge helix, thus playing an inhibitory role (Fig. 1 and Fig. 2C-D, Fig. S3A right). RII.2 (residues 86-105) occupies the space of the DNA template strand (Fig. 2C-D), indicating that RII.2 has to relocate to permit template-strand DNA access into the RNAP active site and for transcription initiation. RII.3 (residues 105-120) extends along the path that is occupied by RNA in the transcribing complex (Fig. 2C-D), suggesting that it will also need to relocate upon RNA synthesis.

Comparisons between σ^{54} and σ^{70} holoenzyme structures reveal that overall they contact similar regions of the RNAP core enzyme (Fig. 3A-B), in agreement with the idea that specific factors unrelated by structure and sequence can be functionally similar (15). However, the relative location of functional domains is completely different. For example, the σ^{54} CBD is located upstream, blocking the RNA exit tunnel (Fig. 3C) while σ_2, the major core binding domain of σ^{70}, contacts the downstream β' region (Fig. 3A-B). The structural differences suggest that σ^{54} CBD, and hence σ^{54}, will have to dissociate or relocate to allow progression from transcription initiation to elongation while σ^{70} can loosely associate with the RNAP core even during transcript elongation, in agreement with earlier biochemical data (16,17). σ^{70} region 4 (σ_4), which recognises the -35 promoter element, occupies the upstream surface blocking the RNA exit channel instead (Fig. 3B).

The inhibitory RI of σ^{54} interacts with RIII across the RNAP cleft, blocking the template strand from entering. On the other hand, $\sigma_{1.1}$ of σ^{70}, which also has an inhibitory role (18), is located in the downstream DNA channel, overlapping with the region occupied by σ^{54} RII.1 (Fig. 3), suggesting that $\sigma_{1.1}$ and RII.1 might play related roles in transcription regulation. However, $\sigma_{1.1}$ connects with σ_2 by only a single flexible linker, allowing the $\sigma_{1.1}$ to move readily from the RNAP cleft (Fig. 1B, Fig. 3B). σ^{54} RII.1 is connected to the RI and hence the RIII-ELH as well as the CBD and the linker that connects RII.1 with the CBD is embedded in the DNA/RNA channel of RNAP (Fig. 2C-D). Due to its topological restraint, σ^{54} RII.1 cannot relocate easily without affecting the conformation of other parts of σ^{54}, RII. 1 will thus block downstream DNA entry.

Notable conformational differences exist between the σ^{70} and σ^{54} holoenzymes in many key modules within the RNAP when superposed on the bridge helix, chosen since the catalytic centre must be conserved (Fig. S3B). The β' coiled-coil, and the whole β' subunit, is rotated, narrowing the downstream DNA channel by as much as 5 Å (Fig. S3B). However, the clamp, which consists of β and β' domains forming the walls of the downstream DNA channel, was shown to adopt multiple conformations in solution (19). The β' coiled-coil forms helical bundles with σ_2 of σ^{70} and helps to stabilise the unpaired non-template DNA strand, and hence the transcription bubble (20) (Fig. S4A). B-linker of TFIIB also interacts with β' coiled-coil (Fig. S4B). In the σ^{54} holoenzyme structure, the β' coiled-coil does not form a helical bundle with σ^{54} (Fig. S4C). However, it is possible that en-route to transcription initiation, this interaction is established, in agreement with our biochemical data (Fig. S4D).

σ^{54} occupies multiple locations along the DNA and RNA path within the RNAP core. These locations are also targeted by other regulatory factors and in other RNAPs. For example, RI and RIII sit across the RNAP cleft, blocking the DNA template strand entry (Fig. 4A). At similar locations, domains 2 and 3 (σ_2 and σ_3) of σ^{70} form a V-shaped wedge that acts as a gate to allow the template strand to enter the active cleft (Fig. 4B) (13, 21). TFIIB also uses two sub-domains, the core binding domain and the B-linker, to occupy similar areas in Pol II (Fig. 4C). This area is thus occupied by σ^{54} to inhibit while by σ^{70} and TFIIB to guide the template strand delivery. Furthermore, σ_2 of σ^{70} contains a number of aromatic residues that are shown to interact with non-template strand, therefore facilitating DNA melting and transcription bubble formation (20). In σ^{54}, there are few aromatic residues in this region (RI and RIII-ELH) that could facilitate DNA melting, in agreement with data showing that although deletion of σ^{54} RI can bypass the requirement of activator proteins, it fails on double-stranded DNA (11). Activator proteins may therefore be directly required for transcription bubble opening. The downstream DNA channel is occupied by both RII.1 of σ^{54} and $\sigma_{1.1}$ of σ^{70} (Fig. 4D). A negatively charged region of TFIIF is also located in the downstream DNA channel of Pol II (22). RII.2 of σ^{54} is located in the channel that is occupied by the template strand DNA in the transcribing RNAP (Fig. 2D). σ^{70} and TFIIB lack equivalent structural features. This area, however, is occupied in Pol I by part of the expander (Fig. 4E), a unique insertion in Pol I compared to Pol II and shown to stabilize an expanded active centre cleft (23, 24) (Fig. 4E). Similar to RII.3, both region 3.2 in σ^{70} (σ finger) and the B-reader in TFIIB are shown to overlap with the space that would be occupied by RNA (Fig. 4D-F) (25). Indeed, RII.3 shares sequence homology with σ, especially the highly conserved DDE motif (Fig. S2). Acidic residues in these elements are proposed to facilitate template DNA loading and RNA separation from DNA, guiding it towards the exit channel (25-28). It is possible that RII.3 also performs similar roles.

Our structure uncovers a diverse range of regulatory strategies utilised by σ^{54} in tightly controlling transcription initiation. These include blocking the template strand from entering the RNAP active cleft by RI and RIII, occupying the downstream DNA channel by RII.1, interfering with the template strand and synthesized RNA by RII.2-RII.3. The position of RI and RIII plays a vital role in these regulatory functions. Activator proteins interact with RI and could relocate RI, RIII-ELH as well as RII, releasing the inhibition posed by some of these structural elements (Fig. S3A) (29, 30). Precisely how activators overcome these

multiple modes of inhibition, and the role of ATP in this process, remains to be determined. Furthermore, we show that although σ^{54}, σ^{70}, TFIIB, TFIIF and Pol I subunits have no sequence or structural similarities, they target the same elements within their respective RNAPs. Our structure and comparisons thus provide clear evidence that regulatory hotspots within RNAPs are functionally conserved. Different transcription factors, irrespective of their structures and sequences, are utilised to target these hotspots in order to exert a fine-tuned transcription regulation strategy (Fig. S5). It will be interesting to see the extent to which additional multi-subunit RNAPs employ these regulatory strategies.

Supplementary Material

Refer to Web version on PubMed Central for supplementary material.

Acknowledgments

We thank Martin Michael, Daniel Bose for their earlier contributions to this project, Andreas Forster, Jiwei Liu and beamline scientists at the Diamond Light Source for their help with data collection, members in XZ and MB's labs for helpful discussion. We thank Dale Wigley, Ray Dixon, Robert Weinzierl and Ramesh Wigneshweraraj for critically reading the manuscript. YY was funded by the Chinese National Science Foundation and the China Scholarship Council. The majority of this work is funded by the UK Biotechnology and Biological Sciences Research Council to XZ and MB. KSM is supported by National Institutes of Health Grant GM087350. YPW is funded by 973 National Key Basic Research Programme (2015CB755700) in China. The atomic coordinate has been deposited in the Protein Data Bank with accession code 5BYH.

References and Notes

1. Mooney RA, Darst SA, Landick R. Sigma and RNA polymerase: an on-again, off-again relationship? Mol Cell. 2005; 20:335–345. [PubMed: 16285916]
2. Feklistov A, Sharon BD, Darst SA, Gross CA. Bacterial sigma factors: a historical, structural, and genomic perspective. Annu Rev Microbiol. 2014; 68:357–376. [PubMed: 25002089]
3. Buck M, Gallegos MT, Studholme DJ, Guo Y, Gralla JD. The bacterial enhancer-dependent sigma(54) (sigma(N)) transcription factor. J Bacteriol. 2000; 182:4129–4136. [PubMed: 10894718]
4. Rappas M, Bose D, Zhang X. Bacterial enhancer-binding proteins: unlocking sigma54-dependent gene transcription. Curr Opin Struct Biol. 2007; 17:110–116. [PubMed: 17157497]
5. Cramer P. Multisubunit RNA polymerases. Curr Opin Struct Biol. 2002; 12:89–97. [PubMed: 11839495]
6. Werner F, Grohmann D. Evolution of multisubunit RNA polymerases in the three domains of life. Nat Rev Microbiol. 2011; 9:85–98. [PubMed: 21233849]
7. Wigneshweraraj SR, Burrows PC, Nechaev S, Zenkin N, Severinov K, Buck M. Regulated communication between the upstream face of RNA polymerase and the beta' subunit jaw domain. EMBO J. 2004; 23:4264–4274. [PubMed: 15470503]
8. Guo Y, Gralla JD. Promoter opening via a DNA fork junction binding activity. Proc Natl Acad Sci U S A. 1998; 95:11655–11660. [PubMed: 9751721]
9. Guo Y, Lew CM, Gralla JD. Promoter opening by sigma(54) and sigma(70) RNA polymerases: sigma factor-directed alterations in the mechanism and tightness of control. Genes Dev. 2000; 14:2242–2255. [PubMed: 10970887]
10. Burrows PC, Wigneshweraraj SR, Buck M. Protein-DNA interactions that govern AAA+ activator-dependent bacterial transcription initiation. J Mol Biol. 2008; 375:43–58. [PubMed: 18005983]
11. Wang JT, Syed A, Gralla JD. Multiple pathways to bypass the enhancer requirement of sigma 54 RNA polymerase: roles for DNA and protein determinants. Proc Natl Acad Sci U S A. 1997; 94:9538–9543. [PubMed: 9275158]

12. Chaney M, Buck M. The sigma 54 DNA-binding domain includes a determinant of enhancer responsiveness. Mol Microbiol. 1999; 33:1200–1209. [PubMed: 10510234]
13. Zuo Y, Steitz TA. Crystal Structures of the E. coli Transcription Initiation Complexes with a Complete Bubble. Mol Cell. 2015; 58:534–540. [PubMed: 25866247]
14. Bose D, et al. Organization of an activator-bound RNA polymerase holoenzyme. Mol Cell. 2008; 32:337–346. [PubMed: 18995832]
15. Decker KB, Hinton DM. Transcription regulation at the core: similarities among bacterial, archaeal, and eukaryotic RNA polymerases. Annu Rev Microbiol. 2013; 67:113–139. [PubMed: 23768203]
16. Bar-Nahum G, Nudler E. Isolation and characterization of sigma(70)-retaining transcription elongation complexes from Escherichia coli. Cell. 2001; 106:443–451. [PubMed: 11525730]
17. Mukhopadhyay J, Kapanidis AN, Mekler V, Kortkhonjia E, Ebright YW, Ebright RH. Translocation of sigma(70) with RNA polymerase during transcription: fluorescence resonance energy transfer assay for movement relative to DNA. Cell. 2001; 106:453–463. [PubMed: 11525731]
18. Bae B, Davis E, Brown D, Campbell EA, Wigneshweraraj S, Darst SA. Phage T7 Gp2 inhibition of Escherichia coli RNA polymerase involves misappropriation of sigma70 domain 1.1. Proc Natl Acad Sci U S A. 2013; 110:19772–19777. [PubMed: 24218560]
19. Chakraborty A, et al. Opening and closing of the bacterial RNA polymerase clamp. Science. 2012; 337:591–595. [PubMed: 22859489]
20. Feklistov A, Darst SA. Structural basis for promoter-10 element recognition by the bacterial RNA polymerase sigma subunit. Cell. 2011; 147:1257–1269. [PubMed: 22136875]
21. Murakami KS, Masuda S, Campbell EA, Muzzin O, Darst SA. Structural basis of transcription initiation: an RNA polymerase holoenzyme-DNA complex. Science. 2002; 296:1285–1290. [PubMed: 12016307]
22. Chen ZA, et al. Architecture of the RNA polymerase II-TFIIF complex revealed by cross-linking and mass spectrometry. EMBO J. 2010; 29:717–726. [PubMed: 20094031]
23. Engel C, Sainsbury S, Cheung AC, Kostrewa D, Cramer P. RNA polymerase I structure and transcription regulation. Nature. 2013; 502:650–655. [PubMed: 24153182]
24. Fernandez-Tornero C, et al. Crystal structure of the 14-subunit RNA polymerase I. Nature. 2013; 502:644–649. [PubMed: 24153184]
25. Kostrewa D, et al. RNA polymerase II-TFIIB structure and mechanism of transcription initiation. Nature. 2009; 462:323–330. [PubMed: 19820686]
26. Sainsbury S, Niesser J, Cramer P. Structure and function of the initially transcribing RNA polymerase II-TFIIB complex. Nature. 2013; 493:437–440. [PubMed: 23151482]
27. Liu X, Bushnell DA, Wang D, Calero G, Kornberg RD. Structure of an RNA polymerase II-TFIIB complex and the transcription initiation mechanism. Science. 2010; 327:206–209. [PubMed: 19965383]
28. Basu RS, et al. Structural basis of transcription initiation by bacterial RNA polymerase holoenzyme. J Biol Chem. 2014; 289:24549–24559. [PubMed: 24973216]
29. Sharma A, et al. Domain movements of the enhancer-dependent sigma factor drive DNA delivery into the RNA polymerase active site: insights from single molecule studies. Nucleic Acids Res. 2014; 42:5177–5190. [PubMed: 24553251]
30. Friedman LJ, Gelles J. Mechanism of transcription initiation at an activator-dependent promoter defined by single-molecule observation. Cell. 2012; 148:679–689. [PubMed: 22341441]
31. Aiba Y, Katayama Y, Hishinuma T, Murakami-Kuroda H, Cui L, Hiramatsu K. Mutation of RNA polymerase beta-subunit gene promotes heterogeneous-to-homogeneous conversion of beta-lactam resistance in methicillin-resistant Staphylococcus aureus. Antimicrob Agents Chemother. 2013; 57:4861–4871. [PubMed: 23877693]
32. Merrick MJ, Gibbins JR. The nucleotide sequence of the nitrogen-regulation gene ntrA of Klebsiella pneumoniae and comparison with conserved features in bacterial RNA polymerase sigma factors. Nucleic Acids Res. 1985; 13:7607–7620. [PubMed: 2999700]

33. Joly N, Zhang N, Buck M. ATPase site architecture is required for self-assembly and remodeling activity of a hexameric AAA+ transcriptional activator. Molecular cell. 2012; 47:484–490. [PubMed: 22789710]
34. Morris L, Cannon W, Claverie-Martin F, Austin S, Buck M. DNA distortion and nucleation of local DNA unwinding within sigma-54 (sigma N) holoenzyme closed promoter complexes. J Biol Chem. 1994; 269:11563–11571. [PubMed: 8157688]
35. Cannon WV, Gallegos MT, Buck M. Isomerization of a binary sigma-promoter DNA complex by transcription activators. Nat Struct Biol. 2000; 7:594–601. [PubMed: 10876247]
36. Kabsch W. Xds. Acta crystallographica Section D, Biological crystallography. 2010; 66:125–132.
37. McCoy AJ, Grosse-Kunstleve RW, Adams PD, Winn MD, Storoni LC, Read RJ. Phaser crystallographic software. Journal of applied crystallography. 2007; 40:658–674. [PubMed: 19461840]
38. Adams PD, et al. PHENIX: a comprehensive Python-based system for macromolecular structure solution. Acta crystallographica. 2010; 66:213–221. [PubMed: 20305355]
39. Emsley P, Lohkamp B, Scott WG, Cowtan K. Features and development of Coot. Acta crystallographica. 2010; 66:486–501.
40. Murshudov GN, et al. REFMAC5 for the refinement of macromolecular crystal structures. Acta crystallographica. 2011; 67:355–367.
41. Blanc E, Roversi P, Vonrhein C, Flensburg C, Lea SM, Bricogne G. Refinement of severely incomplete structures with maximum likelihood in BUSTER-TNT. Acta crystallographica. 2004; 60:2210–2221.
42. Chlenov M, Masuda S, Murakami KS, Nikiforov V, Darst SA, Mustaev A. Structure and function of lineage-specific sequence insertions in the bacterial RNA polymerase beta' subunit. J Mol Biol. 2005; 353:138–154. [PubMed: 16154587]
43. Knutson BA, Luo J, Ranish J, Hahn S. Architecture of the Saccharomyces cerevisiae RNA polymerase I Core Factor complex. Nat Struct Mol Biol. 2014; 21:810–816. [PubMed: 25132180]

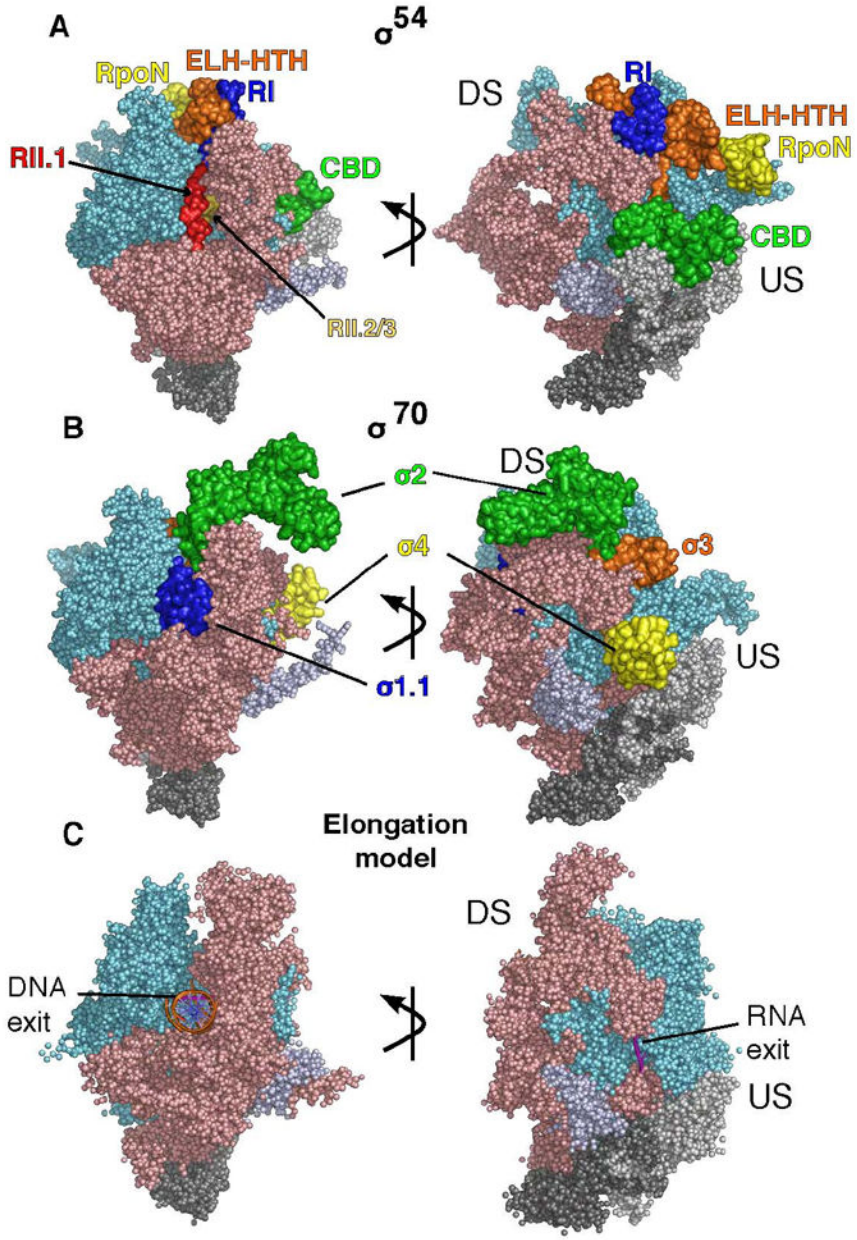

Figure 1. Structure of complete RNAP-σ^{54}

(A) Structure and schematic diagram of σ^{54}. (**B)** Structure of σ^{70} (PDB 4IGC) with similar functional domains colored accordingly. (**C)** Holoenzyme in different orientations, RNAP core in cylinders. β-cyan, β'-salmon pink, α-grey, ω-pale blue, σ^{54} in ribbon and colored as in (**A**), **DS** represents downstream, **US** represents upstream. (**D)** Residues of β and β' subunits that are crosslinked to σ^{54} are mapped onto the structure and colored in yellow (**E)** Electron density map and structural model of RNAP-σ^{54}-DNA.

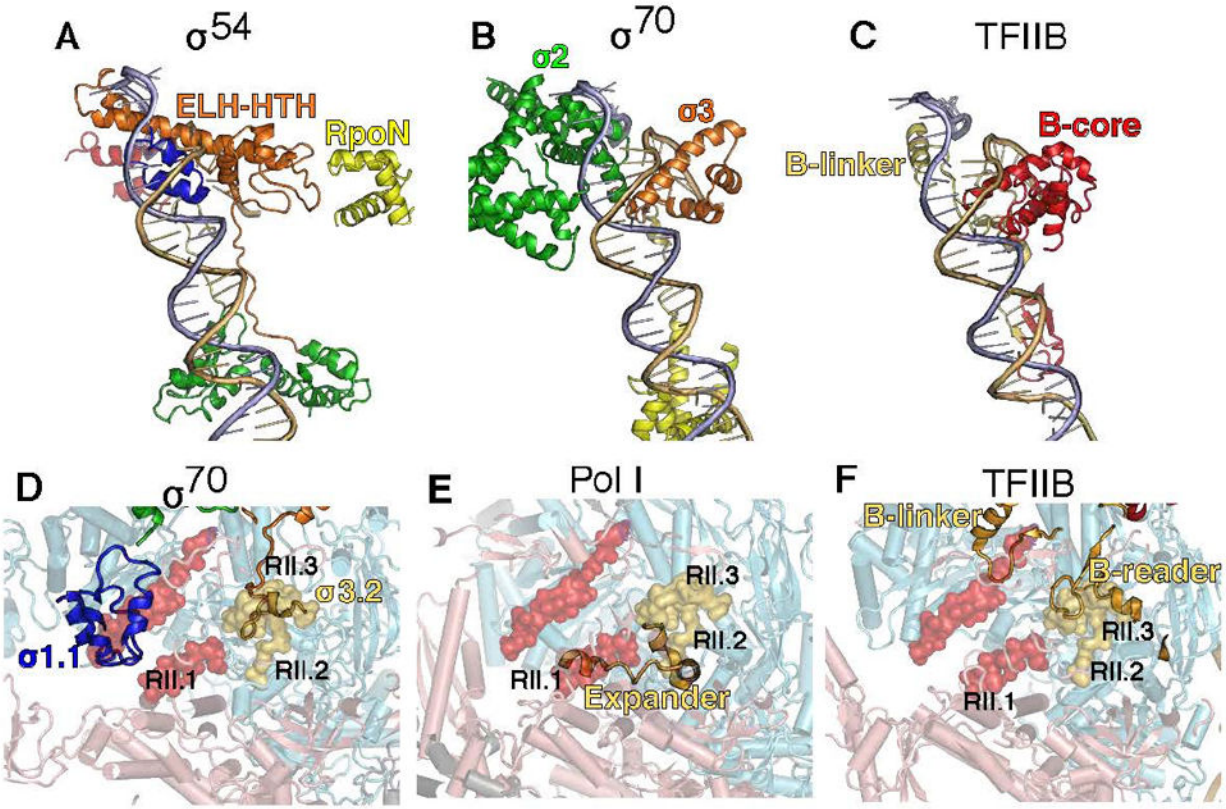

Figure 2. Functional domains of σ^{54} and interactions with RNAP core

(**A)** Detailed view of the CBD and RNAP interactions. **(B)** RI and RIII, **(C)** DNA-RNA channels, DNA-orange, RNA-magenta and **(D)** Overlay with RII.1, RII.2 and RII.3.

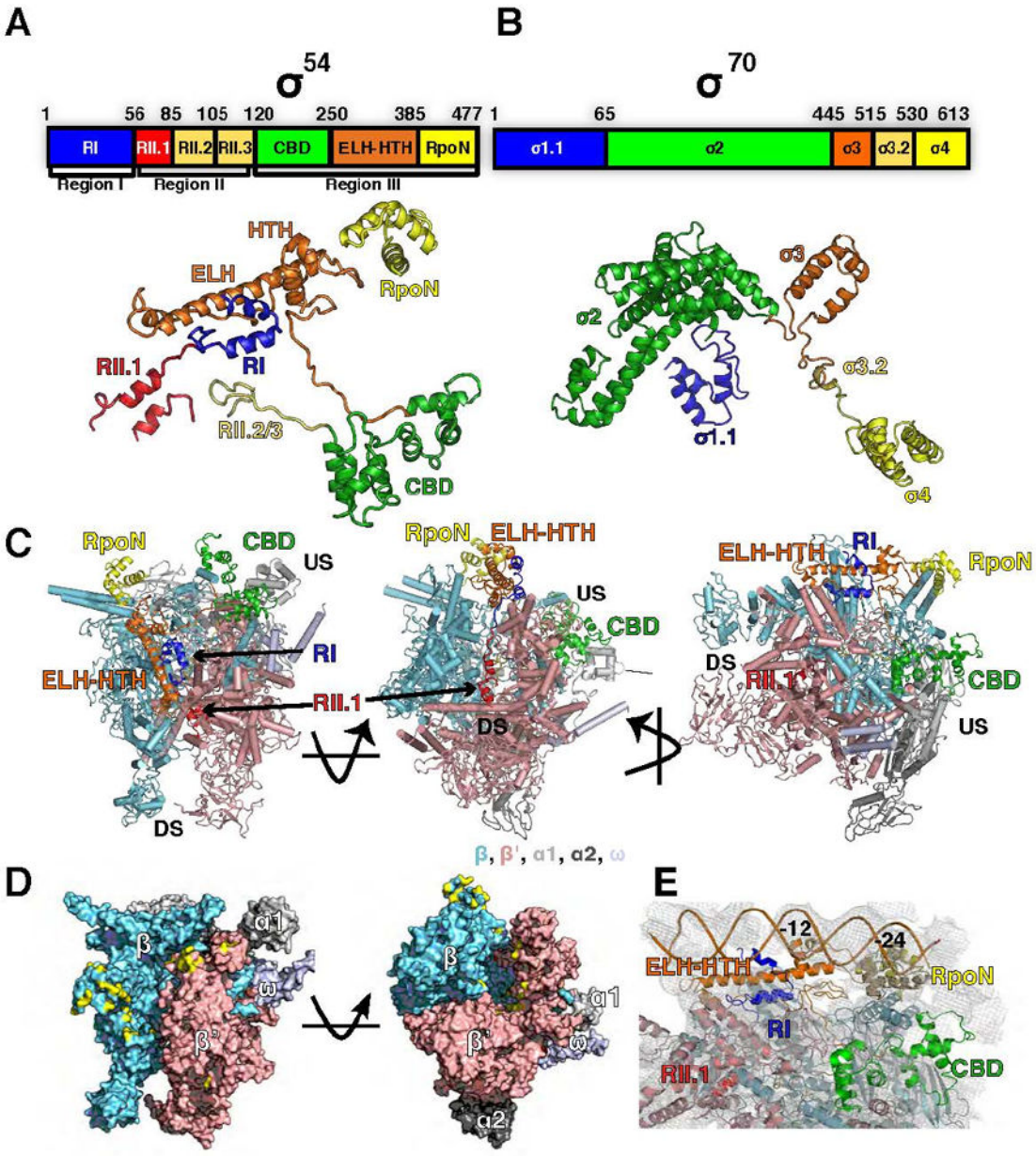

Figure 3. Comparisons of σ^{54} and σ^{70} holoenzymes

(**A**) RNAP-σ^{54} with RNAP displayed as spheres and σ^{54} as surface. **(B)** RNAP-σ^{70}, same view as in (**A**). (**C**) Elongation complex (PDB code 2O5J).

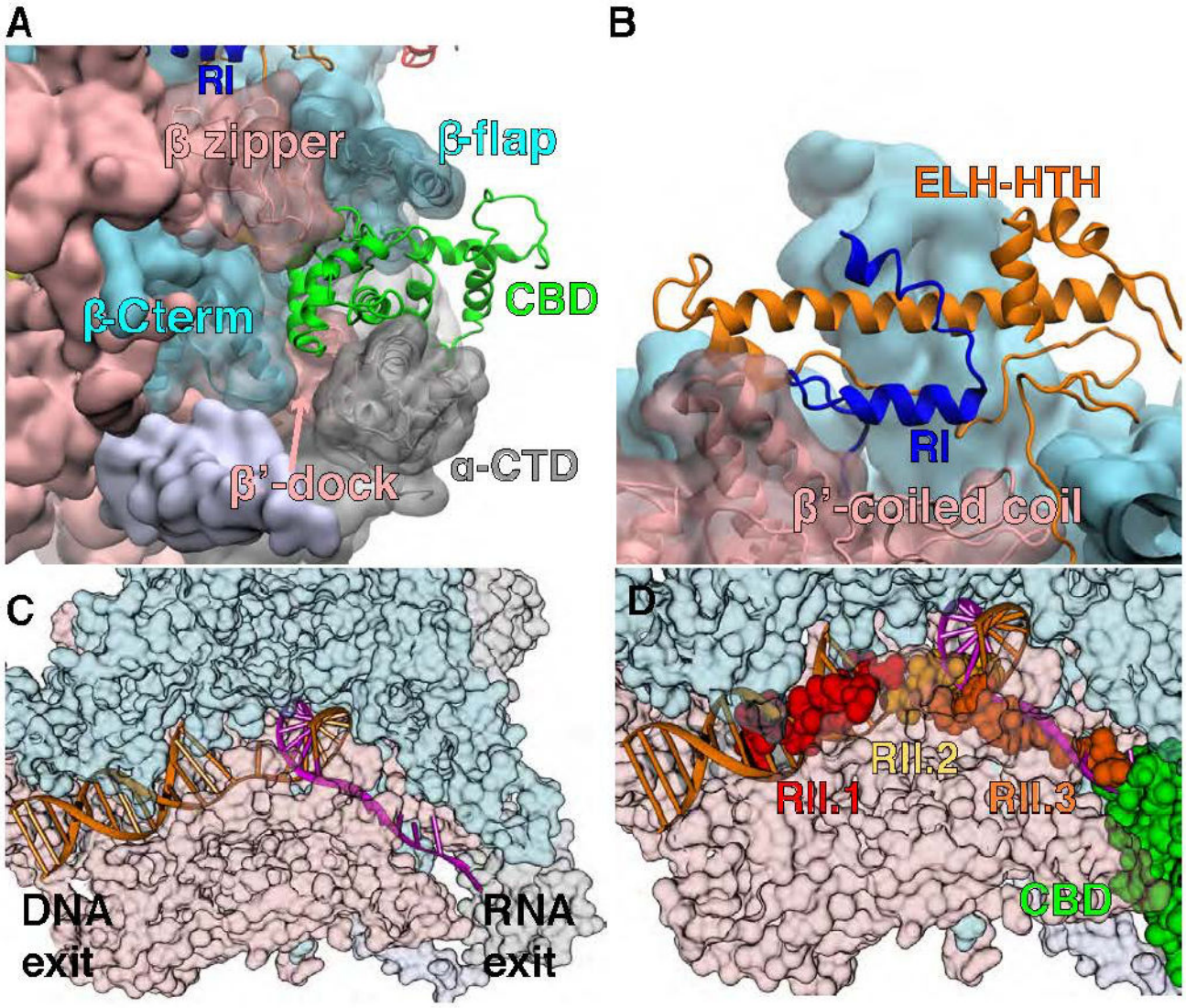

Figure 4. Regulatory elements of σ^{54} and comparison with σ^{70}, TFIIB and Pol I

(A) σ^{54} **(B)** σ^{70} and (**C**) TFIIB in relation to template strand (gold) as defined in the complex with a full transcription bubble (4YLN). (**D-F**) Comparison of σ^{54} with σ^{70}, Pol I (4C2M) and TFIIB (4BBS) in the RNAP DNA-RNA channel; structures are superposed on the bridge helix. σ^{54} represented as spheres while σ^{70}, TFIIB and Pol I expander as ribbons, RNAPs as cylinders.